

Numerical simulation of the effective permittivity of low-density polyethylene composite filled by carbon black

eISSN 2514-3255

Received on 14th April 2019

Revised 1st July 2019

Accepted on 9th July 2019

E-First on 26th July 2019

doi: 10.1049/iet-nde.2019.0017

www.ietdl.org

Sohrab Azizi¹ ✉, Éric David¹, Michel F. Fréchette¹, Claudiane M. Ouellet-Plamondon¹

¹École de technologie supérieure (Université du Québec), 1100 Notre-Dame St W, Montréal, QC H3C 1K3, Canada

✉ E-mail: sohrab.azizi.1@ens.etsmtl.ca

Abstract: The effective permittivity of low-density polyethylene with the conductive carbon black (CB) was modelled by COMSOL. The impact of CB content on the electric properties of the composites with different geometry of the inclusions was investigated. The modelling outcomes evidenced that the simulation was in good agreement with the experiment results at low-filler concentration. The effect of moisture on the effective permittivity of the composites was also investigated. A thin layer of adsorbed water on the surface of the CB particles was found to significantly increase the conductivity, which is in agreement with experimental results.

1 Introduction

Significant attention is paid to binary or multicomponent composite materials comprising conductive particles due to their suitable electrical properties for electrical applications. Numerous experimental researches have been performed to investigate the effect of the inclusion of conductive particles on the effective permittivity of the composites [1–6]. Although the conducted experiments are worthwhile and valuable, those researches are time-consuming and expensive. Thus, numerical and analytical modelling of the composites could be an appropriate way to predict and estimate the electrical properties of composites. The composites are formed from a matrix loaded with one or more types of inclusions. These materials were considered as heterogeneous systems with their effective electrical properties (e.g. effective complex permittivity) being highly dependent on the filler geometry [7, 8], filler content, filler dispersion and distribution [6, 9], interfacial interaction between matrix and particles [10, 11] and the inherent properties of the inclusions and the matrix [12–18]. Furthermore, the distribution of the distance between the particles, and the number of contact points between them are two determining parameters for the effective electrical properties [8, 19–21]. Taking into account the above-mentioned parameters, the electrical properties of the composites such as the dielectric response can be somehow predicted by varieties of theories and models. For instance, the electrical properties of the composites with conductive particles can be anticipated by providing the actual geometry and/or the spatial arrangement of the inclusions in the matrix.

The effective permittivity of the composites was estimated and reported based on the filler orientation within the matrix. It was suggested that the minimum value could be achieved by a laminated structure for which the phases are in series as follows [17, 22, 23]:

$$\epsilon_{\min, C} = \frac{\epsilon_f \epsilon_m}{\epsilon_f \varphi_f + \epsilon_m \varphi_m} \quad (1)$$

and that the maximum value is obtained when the laminates are in parallel (with respect to the electrical field) as follows:

$$\epsilon_{\max, C} = \epsilon_f \varphi_f + \epsilon_m \varphi_m \quad (2)$$

where ϵ represents the effective permittivity, φ the volume fraction, the indexes f and m corresponding to the filler and matrix, respectively. The aforementioned models give a global viewpoint

of the effective permittivity of the composite but do not provide the exact bounds. In another suggested model, Vargas-Bernal and his co-workers simulated the DC electrical conductivity of binary composites using Kirkpatrick's model with more influential parameters. Based on this model, the DC electrical conductivity of the composite depends on the probability of the contacts between particles within the composite, which leads to an alteration of the property of the matter from an insulating to a conductive one based on a power law as follows:

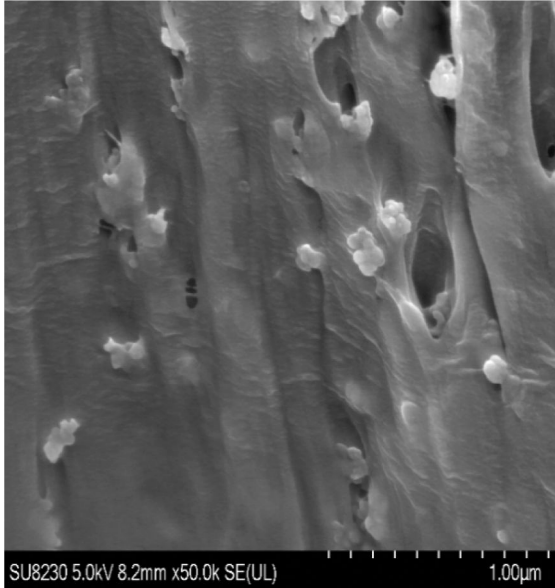
$$\sigma_{DC} = k (\varphi - \varphi_c)^t \quad (3)$$

where σ_{DC} is the conductivity of the composite, φ is the volume filler concentration and φ_c is the volume concentration at the critical concentration, k is a constant and t is the critical exponent [24, 25]. The AC conductivity of polymethyl methacrylate with antimony tin oxide filler was modelled and estimated by Jin and Gerhardt [26]. Their findings revealed that a perfect network of the connected fillers is more conductive than a random path connected. Both mentioned arrangements were also more conductive than the one with randomly distributed particles below the percolation threshold. The macroscopic electrical conductivity of carbon nanotube (CNT)–polymer composite materials was simulated using a multiscale approach by Shenogin *et al.* [21]. They reported that the metallisation of the CNT–CNT contact-point leads to 150–500 times improvement in electrical conductivity. A Monte–Carlo model was used by Coelho *et al.* [27] to estimate the percolation threshold of the individual and hybrid composite materials with carbon black (CB) and CNT particles. Their modelling results indicated that the percolation threshold of the composites including an individual filler is corresponding to the experiments. However, for the multi-particle composites, the experimental results were not in good agreement with the modelling. Nevertheless, the best arrangement of the inclusion with the lowest percolation threshold was obtained.

In this work, the effective permittivity of the low-density polyethylene (LDPE)-based composites was analysed numerically. The structure of the composite was designed and modelled according to the real morphology of the composites obtained by scanning electron microscopy (SEM) images in our experimental work [28]. The simulations were conducted for LDPE composites with CB fillers with different arrangements (ideal and real orientation). The effect of the absorbed moisture by CB filler on the electrical properties of the composites was also investigated. The obtained results were compared with the experiments.

Table 1 Electrical properties of the materials used for the simulation

Material	Electrical conductivity, S/m	Complex permittivity at 10^6 Hz including the contribution of the conductivity	Reference for the obtained data
PE	10^{-15}	$\epsilon^* = 2.3$	our measurement
CB	100	$\epsilon^* = 30 - 1.80 \times 10^6 i$	our measurement
deionised water	5.5×10^{-6}	$\epsilon^* = 80 - 0.0988 i$	[33]

**Fig. 1** SEM micrograph of LDPE/CB 15 wt% at 50K magnification

2 Models and methods

The effective permittivity of the composite was evaluated based on the filler orientation and arrangement. The modelling was also compared to the effect of the particle size on effective permittivity for the composites with the same filler concentration.

A periodic geometry was chosen thus neglecting edge effect at boundary conditions. In the three-dimensional representative element, the four parallel surface boundaries along the Z-direction were selected as periodic surfaces. The applied electrical field was set along the Z-direction by setting to 5 V the potential of the top surface and to zero the potential of the bottom surface. The modelling was performed in the frequency domain with a harmonic electrical field condition. The effective permittivity of the composite was obtained from (4) [29–31]

$$\epsilon_c = \frac{\langle D \rangle}{\langle E \rangle \epsilon_0} \quad (4)$$

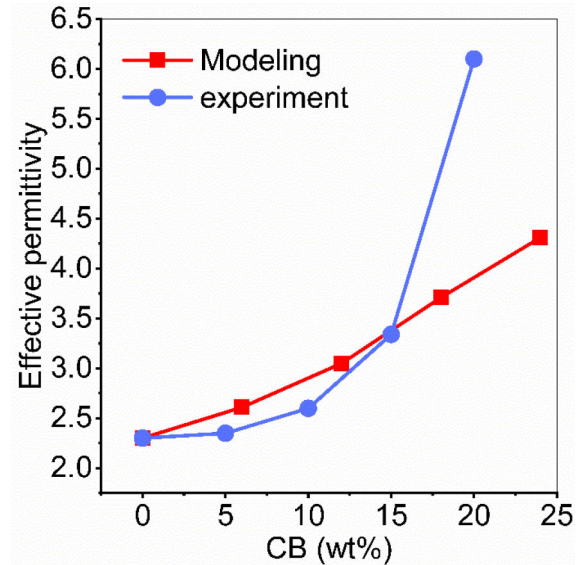
where ϵ_c is the composite effective permittivity, D is the average electric flux density, $\langle E \rangle$ is the average of the electrical field over the selected cubic element and ϵ_0 is the vacuum permittivity. It should be noted that these three values are in general complex values.

In the present study, conductive CB with an electrical conductivity of 100 (S/m) and a dielectric constant (real part of the complex permittivity) of $\epsilon = 30$ [32] at the frequency of 10^6 Hz was used for the numerical simulation. The electrical properties for the other phases are given in Table 1. The imaginary part of the permittivity (other than the one coming from the conductivity) for polyethylene (PE) and CB was assumed to be negligible for the investigated frequency range.

3 Results and discussion

3.1 Filler content

In order to understand the dispersion and distributions of CB particles in composite's structure, a cross-section SEM image of the

**Fig. 2** Effective permittivity of the LDPE/CB composite at different filler contents (CB without moisture, with a random dispersion)

LDPE/CB composite containing 15 wt.% of CB was taken and is shown in Fig. 1. As illustrated, the CB particles are characterised by a spheroidal geometry. Furthermore, the CB particles seem to be randomly distributed within the composite. The effective permittivity of the composite as a function of the filler fraction (weight %) is shown in Fig. 2. As is shown, the effective permittivity of the composites was found to increase with the addition of the conductive CB. The computed values of the permittivity were found to be in reasonably good agreement up to 15 wt% and then were clearly underestimating the experimental values. In fact, at this critical filler concentration (percolation threshold), the conductivity of the composite was also found to sharply increase. In order to compare the numerical results with experimental findings, and to convert the volume fraction used in the numerical simulations in weight fractions, we considered the bulk density of LDPE and CB as 920 and 1120 kg/m³, respectively. The effective permittivity of simulated composites at low filler contents featured closer values to the experimental results, but at high filler contents, the difference was noticeable, which means the modelling cannot correctly predict the electrical properties of the composites at high filler contents. The surface plots of the magnitude of the electric displacement field within LDPE/CB composites are shown in Fig. 3. An enhancement of the electrical field was found at the interface of inclusion medium, which is in good agreement with the analytic solution of the single inclusion problem. In addition, decreasing the particles size (and increasing their number to keep the same volume fraction) throughout the composites was found to increase the electric displacement field in which the maximum electric field density was found in the case of 20 vol.% (4.2×10^{-3} C/m²). The higher electric displacement field can be addressed by the following equation [34]:

$$J = \int_0^{D_{\max}} E dD \quad (5)$$

where J denotes the energy storage density, E stands for the electric field, D is the electric displacement and D_{\max} represents the highest value of the electrical displacement. Therefore, based on (5), the

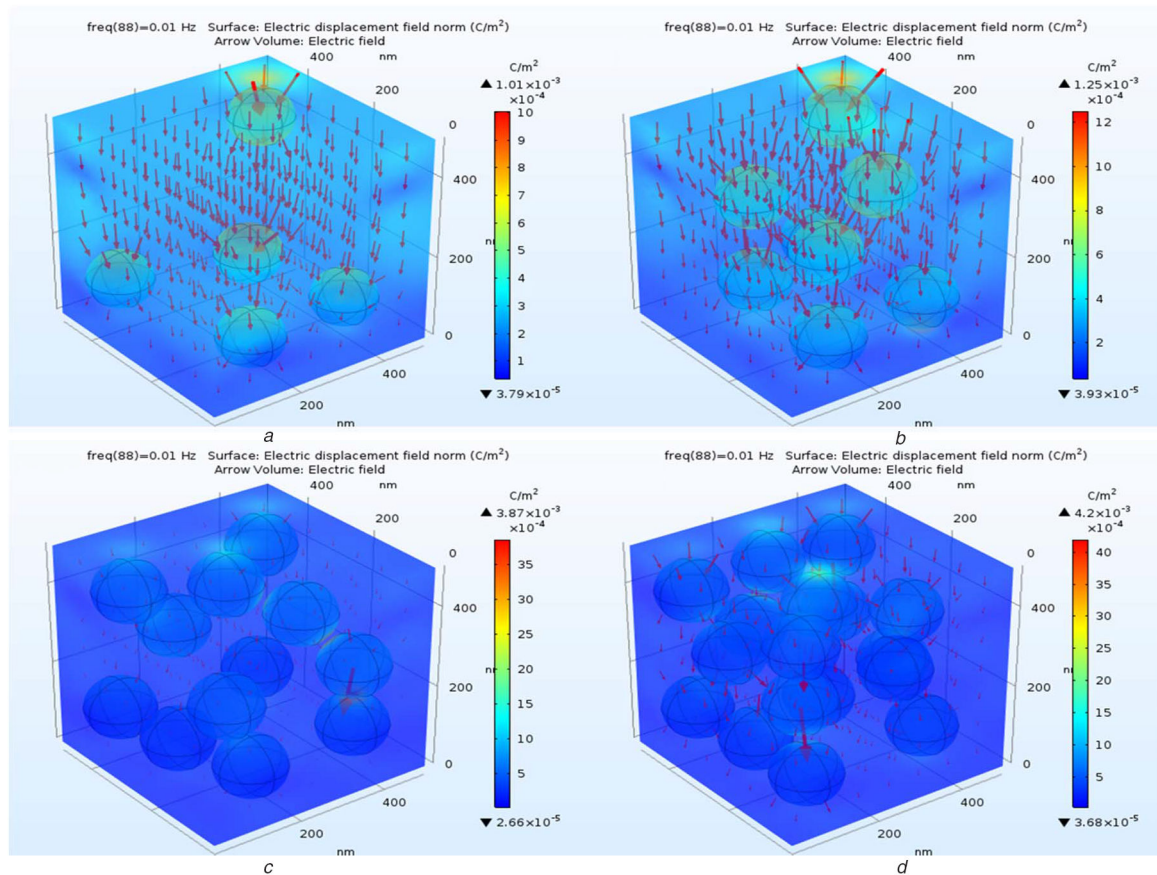


Fig. 3 Surface plots of the electric displacement field norm of LDPE/CB composites with a random distribution of particles comprising of (a) 5 vol.% of CB, (b) 10 vol.% of CB, (c) 15 vol.% of CB, (d) 20 vol.% of CB

Table 2 Effective permittivity of the LDPE/CB composites containing 10 vol.% filler content with different particle distribution

Particle number	Particle radius, nm	Effective permittivity (ϵ)	
		Ordered dispersion	Random dispersion
1	144	3.05	3.03
8	72	3.06	3.02
27	48	3.07	3.06
64	36	3.07	3.09

rise of the total energy of the material would intensify the electric displacement field [35].

3.2 Orientation effect on the permittivity of the composites with constant filler content

The role of particle distribution and particle size on the electrical properties of the composite was studied. In this respect, the LDPE/CB 10 vol.% was selected, and the CB particles were either distributed randomly or placed in a regular order to form a symmetrical pattern. As can be seen in Table 2 at the same volume fraction of CB and a different number of particles and arrangement did not lead to a significant change in effective permittivity and the resulting electrical properties remained essentially unchanged. The surface plots of the magnitude of the electrical field of the modelled LDPE/CB10% with ordered and random filler distribution are illustrated in Figs. 4 and 5, respectively. An increase in the electrical field is observed on the surface of the particles, particularly in the Z-direction. At the same filler content, the highest value of the electric field magnitude was observed for the composite containing 64 particles randomly dispersed. The effective permittivity of the LDPE/CB 10 vol.% with 64 particles is slightly greater than the others with the same volume content of the CB.

The role of particle aggregation in the electrical properties of the LDPE/CB composites was modelled using 10 vol.% of CB filler with and without aggregation formation in a random

orientation as shown in Figs. 5c and 6. The intra-connection between the CB particles in the aggregated regions resulted in a higher effective permittivity of 3.22 with respect to 3.06 of the LDPE/CB 10 vol.% without any connection between the particles. The growth in effective permittivity of composites has been shown in experimentally studies thanks to the intra-connection of conductive particles [36–39]. Similarly, a higher electric field on the surface of the particles was observed for the LDPE/CB composite with 10 vol.% for some locally aggregated regions (see Fig. 6).

3.3 Effect of moisture

The hydrophilic behaviour of CB particle was experimentally found to have a significant impact on the composites electrical properties. In this section, a thin membrane of moisture was created around the particles and the role of moisture on the effective permittivity of composites was evaluated. The effective permittivity of LDPE/CB 10 vol.% with and without moisture as a function of the number of particles is shown in Fig. 7. The water with effective permittivity of 80 and significant electrical conductivity (5.5×10^{-6} S/m) with respect to the insulating polymer engendered a significant synergies effect on the effective permittivity of the composites. Thus, a significant increase in the effective permittivity of the composites was obtained. Furthermore, the composites with more particles were more susceptible to absorb moisture, and more moisture caused a significant increase in

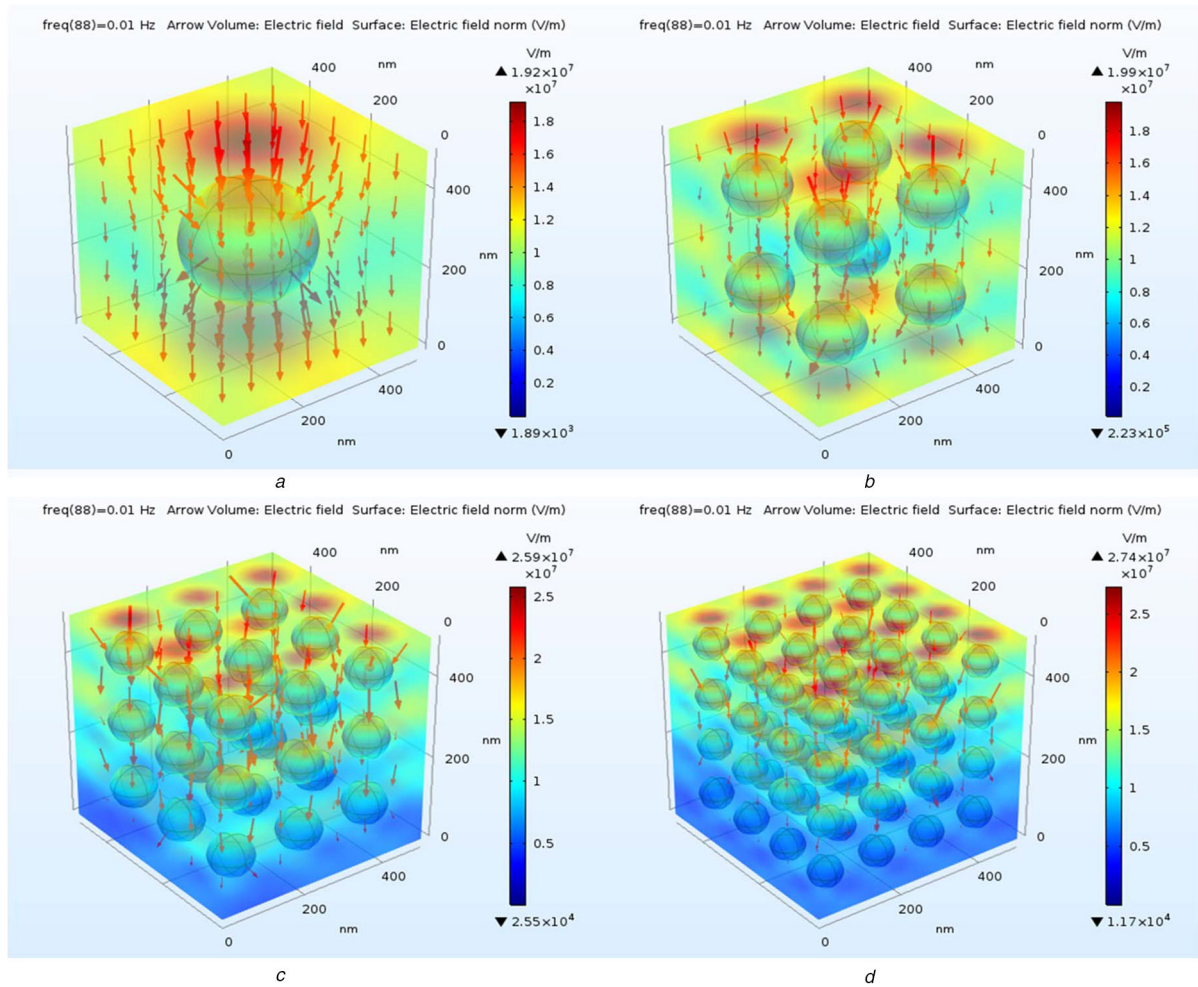


Fig. 4 Surface plots of electric field norm of the LDPE/CB 10 vol.% composite with different particles number
(a) 1 with ordered distribution, (b) 8 with ordered distribution, (c) 27 with ordered distribution, (d) 64 with ordered distribution

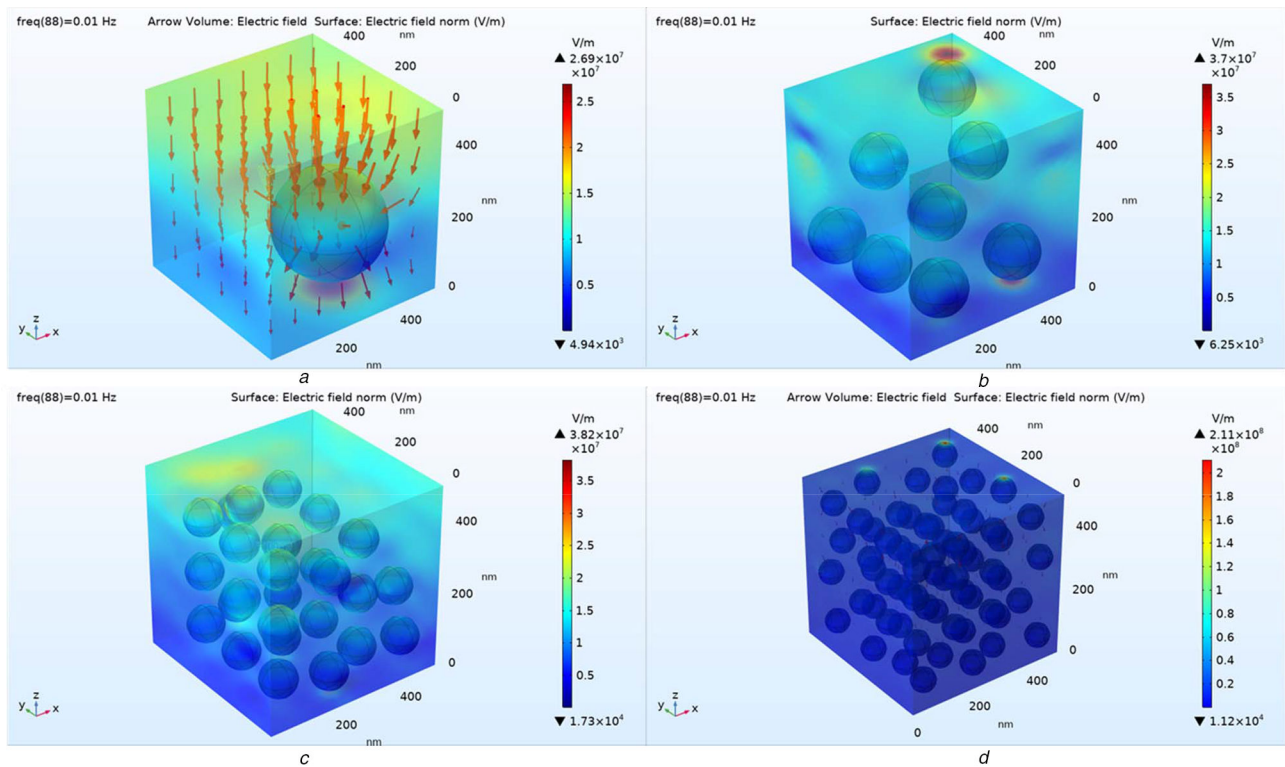


Fig. 5 Surface plots of electric field norm of the LDPE/CB 10 vol.% composite with different particles number
(a) 1, (b) 8, (c) 27, (d) 64 with random distribution at the applied electric field of 5 V

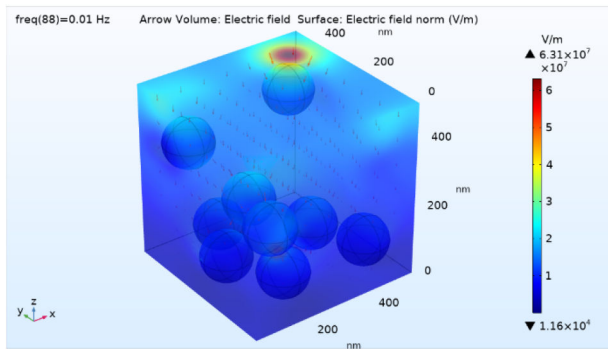


Fig. 6 Surface plot of the electric field norm of the LDPE/CB 10 vol.% composite with nine particles in a aggregated state

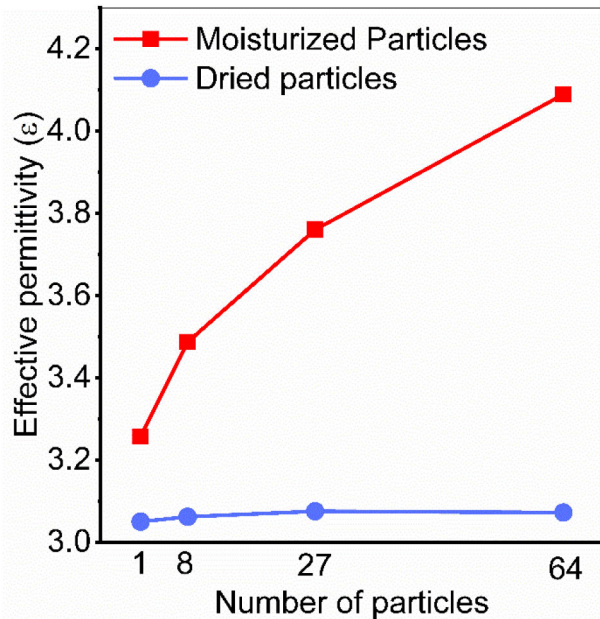


Fig. 7 Numerical effective permittivity of LDPE/CB 10 vol.% composite with different dried and moisturized particles

effective permittivity. The experimental findings [28] are in good agreement with the conducted BDS at two successive runs. Performing a BDS measurement at room temperature after exposure to 100°C to remove absorbed moisture allowed to clarify the role of absorbed water, since the resulting permittivity of composites was decreased.

4 Conclusions

The nanostructure LDPE composite with CB filler was designed, and the effective permittivity was estimated by finite-element modelling. Filler geometry and arrangement were found to have a significant influence on the electrical properties. Moisture absorption by CB particles was found to increase the effective permittivity of the LDPE/CB composite. The effective permittivity of the LDPE composite obtained by numerical modelling was found to be in good agreement with the experimental results at low filler content.

5 Acknowledgment

The authors would like to thank École de technologie supérieure (ÉTS) and Natural Sciences and Engineering Research Council of Canada (NSERC) for their support.

6 References

- [1] Nilsson, F., Krueckel, J., Schubert, D.W., *et al.*: 'Simulating the effective electric conductivity of polymer composites with high aspect ratio fillers', *Compos. Sci. Technol.*, 2016, **132**, pp. 16–23
- [2] Cai, Z., Wang, X., Luo, B., *et al.*: 'Nanocomposites with enhanced dielectric permittivity and breakdown strength by microstructure design of nanofillers', *Compos. Sci. Technol.*, 2017, **151**, pp. 109–114
- [3] Nilsson, F., Gedde, U., Hedenqvist, M.: 'Modelling the relative permittivity of anisotropic insulating composites', *Compos. Sci. Technol.*, 2011, **71**, pp. 216–221
- [4] Serdyuk, Y.V., Podoltsev, A.D., Gubanski, S.M.: 'Numerical simulations of dielectric properties of composite material with periodic structure', *J. Electrostat.*, 2005, **63**, pp. 1073–1091
- [5] Moalleminejad, M., Chung, D.: 'Dielectric constant and electrical conductivity of carbon black as an electrically conductive additive in a manganese-dioxide electrochemical electrode, and their dependence on electrolyte permeation', *Carbon*, 2015, **91**, pp. 76–87
- [6] Azizi, S., David, É., Fréchette, M., *et al.*: 'Improving high voltage cables using LDPE/CB conductive composites', *Substance ÉTS*, 2019
- [7] Huang, Y., Krentz, T.M., Nelson, J.K., *et al.*: 'Prediction of interface dielectric relaxations in bimodal brush functionalized epoxy nanodielectrics by finite element analysis method'. 2014 IEEE Conf. on Electrical Insulation and Dielectric Phenomena (CEIDP), Des Moines, IO, USA, 2014, pp. 748–751
- [8] Barzegar-Parizi, S., Rejaei, B.J.I.M.: 'Antennas, propagation calculation of effective parameters of high permittivity integrated artificial dielectrics', *IET Microwaves, Antennas & Propagation*, 2015, **9**, pp. 1287–1296
- [9] Bao, W., Meguid, S., Zhu, Z., *et al.*: 'Modeling electrical conductivities of nanocomposites with aligned carbon nanotubes', *Nanotechnology*, 2011, **22**, p. 485704
- [10] Amini, A., Bahreyni, B.: 'Behavioral model for electrical response and strain sensitivity of nanotube-based nanocomposite materials', *J. Vac. Sci. Technol. B, Microelectron. Nanometer Struct.*, 2012, **30**, p. 022001
- [11] Xu, J., Zhong, W., Yao, W.: 'Modeling of conductivity in carbon fiber-reinforced cement-based composite', *J. Mater. Sci.*, 2010, **45**, pp. 3538–3546
- [12] Wang, Z., Nelson, J.K., Hillborg, H., *et al.*: 'Dielectric constant and breakdown strength of polymer composites with high aspect ratio fillers studied by finite element models', *Compos. Sci. Technol.*, 2013, **76**, pp. 29–36
- [13] Tanaka, T., Kozako, M., Fuse, N., *et al.*: 'Proposal of a multi-core model for polymer nanocomposite dielectrics', *IEEE Trans. Dielectr. Electr. Insul.*, 2005, **12**, pp. 669–681
- [14] Atif, R., Inam, F.: 'Modeling and simulation of graphene based polymer nanocomposites: advances in the last decade', *Graphene*, 2016, **5**, pp. 96–142
- [15] Zare, Y., Rhee, K.Y.: 'Development of a model for electrical conductivity of polymer/graphene nanocomposites assuming interphase and tunneling regions in conductive networks', *Ind. Eng. Chem. Res.*, 2017, **56**, pp. 9107–9115
- [16] Mora, A., Han, F., Lubineau, G.: 'Computational modeling of electrically conductive networks formed by graphene nanoplatelet-carbon nanotube hybrid particles', *Model. Simul. Mater. Sci. Eng.*, 2018, **26**, p. 035010
- [17] Jylha, L., Sihvola, A.H.: 'Numerical modeling of disordered mixture using pseudorandom simulations', *IEEE Trans. Geosci. Remote Sens.*, 2005, **43**, pp. 59–64
- [18] Lenler-Eriksen, H.-R., Meincke, P.J.E.L.: 'Estimation of complex permittivity using loop antenna', *IET Microwaves, Antennas & Propagation*, 2004, **40**, pp. 285–287
- [19] Louis, P., Gokhale, A.: 'Computer simulation of spatial arrangement and connectivity of particles in three-dimensional microstructure: application to model electrical conductivity of polymer matrix composite', *Acta Mater.*, 1996, **44**, pp. 1519–1528
- [20] Hoang, L.T., Leung, S.N., Zhu, Z.H.: 'Eliminating common biases in modelling the electrical conductivity of carbon nanotube-polymer nanocomposites', *Phys. Chem. Chem. Phys.*, 2018, **20**, pp. 13118–13121
- [21] Shenogin, S., Lee, J., Voevodin, A.A., *et al.*: 'Multiscale modeling of electrical transport in carbon nanotube-metal-polymer composite materials'. 24th AIAA/AHS Adaptive Structures Conf., San Diego, CA, USA, 2016, p. 0822
- [22] Torquato, S.: 'Modeling of physical properties of composite materials', *Int. J. Solids Struct.*, 2000, **37**, pp. 411–422
- [23] Sihvola, A.: 'Mixing rules with complex dielectric coefficients', *Subsurf. Sens. Technol. Appl.*, 2000, **1**, pp. 393–415
- [24] Vargas-Bernal, R., Herrera-Pérez, G., Calixto-Olalde, M., *et al.*: 'Analysis of DC electrical conductivity models of carbon nanotube-polymer composites with potential application to nanometric electronic devices', *J. Electr. Comput. Eng.*, 2013, **2013**
- [25] Stepashkina, A., Tsobkallo, E., Alyoshin, A.: 'Electrical conductivity modeling and research of polypropylene composites filled with carbon black', *J. Phys., Conf. Ser.*, 2014, **572**, p. 012032
- [26] Jin, Y., Gerhardt, R.A.: 'Percolation and electrical conductivity modeling of novel microstructured insulator-conductor nanocomposites fabricated from PMMA and ATO', *MRS Online Proc. Libr. Arch.*, 2014, **1692**
- [27] Coelho, P.H.S.L., Armellini, V.A.D., Morales, A.R.: 'Assessment of percolation threshold simulation for individual and hybrid nanocomposites of carbon nanotubes and carbon black', *Mater. Res.*, 2017, **20**, pp. 1638–1649
- [28] Azizi, S., David, É., Fréchette, M.F., *et al.*: 'Electrical and thermal phenomena in low-density polyethylene/carbon black composites near the percolation threshold', *J. Appl. Polym. Sci.*, 2018, **136**, p. 47043
- [29] Myroshnychenko, V., Brosseau, C.: 'Finite-element method for calculation of the effective permittivity of random inhomogeneous media', *Phys. Rev. E*, 2005, **71**, p. 016701

- [30] Zazoum, B., David, E., Ngó, A.D.: 'Simulation and modeling of polyethylene/clay nanocomposite for dielectric application', *Trans. Electr. Electron. Mater.*, 2014, **15**, pp. 175–181
- [31] Venkatesulu, B., Jonsson, B.L.G., Edin, H., *et al.*: 'Modeling of insulating nanocomposites-electric and temperature fields', *IEEE Trans. Dielectr. Electr. Insul.*, 2013, **20**, pp. 177–184
- [32] Hotta, M., Hayashi, M., Lanagan, M.T., *et al.*: 'Complex permittivity of graphite, carbon black and coal powders in the ranges of X-band frequencies (8.2 to 12.4 GHz) and between 1 and 10 GHz', *ISIJ Int.*, 2011, **51**, pp. 1766–1772
- [33] Renaudot, R., Daunay, B., Kumemura, M., *et al.*: 'Optimized micro devices for liquid-dielectrophoresis (LDEP) actuation of conductive solutions', *Sens. Actuators B*, 2013, **177**, pp. 620–626
- [34] Dang, Z.M., Yuan, J.K., Yao, S.H., *et al.*: 'Flexible nanodielectric materials with high permittivity for power energy storage', *Adv. Mater.*, 2013, **25**, pp. 6334–6365
- [35] Cai, Z., Wang, X., Luo, B., *et al.*: 'Dielectric response and breakdown behavior of polymer–ceramic nanocomposites: the effect of nanoparticle distribution', *Compos. Sci. Technol.*, 2017, **145**, pp. 105–113
- [36] Azizi, S., David, E., Fréchette, M.F., *et al.*: 'Electrical and thermal conductivity of ethylene vinyl acetate composite with graphene and carbon black filler', *Polym. Test.*, 2018, **72**, pp. 24–31
- [37] Azizi, S., Ouellet-Plamondon, C., David, E., *et al.*: 'Electrical and thermal properties of low-density polyethylene/graphene-like composite'. 2017 IEEE Conf. on Electrical Insulation and Dielectric Phenomenon (CEIDP), 2017, pp. 517–520
- [38] Azizi, S., Ouellet-Plamondon, C., David, E., *et al.*: 'Electric response and thermal properties of ethylene vinyl acetate/graphene-based composite'. 2018 IEEE Conf. on Electrical Insulation and Dielectric Phenomena (CEIDP), Cancun, Mexico, 2018, pp. 62–65
- [39] Azizi, S., Azizi, M., Sabetzadeh, M.: 'The role of multiwalled carbon nanotubes in the mechanical, thermal, rheological, and electrical properties of PP/PLA/MWCNTs nanocomposites', *J. Compos. Sci.*, 2019, **3**, p.64